*Proceedings of the*
*Annual Stability Conference*
*Structural Stability Research Council*
*San Antonio, Texas, March 19-22, 2024*

# Methods to improve the accuracy and efficiency of geometric nonlinear analyses of steel frames

Nadine Faramawi[1], Barry T. Rosson[2]

## Abstract

The analysis of steel frames that consider second-order effects requires the solution of a nonlinear system of equilibrium equations. Typical numerical solution techniques involve the use of a geometric stiffness matrix and load increments to determine the nodal displacements and member forces in the frame's deformed configuration. This paper investigates the development and performance of a new higher-order geometric stiffness matrix that more closely approximates the theoretically derived stiffness coefficients. Factors that influence the accuracy and efficiency of the solution scheme are studied using two columns, two braced frames, and four unbraced frames. A linear relationship is discovered between the amplification factor and the number of load increments that are needed to limit the relative error to one percent when performing a second-order elastic analysis with a predictor-corrector solution scheme. A simple equation is proposed for design purposes that uses an approximate amplification factor based on the elastic critical buckling load ratio to determine the minimum number of load increments. Twenty-two benchmark frames are used to verify the proposed design equation. Discussion is provided on when the new geometric stiffness matrix can be used to reduce the required number of elements and on the use of the new linear equation to determine the required minimum number of load increments.

## 1. Introduction

The strength requirements of frames are often evaluated considering geometric nonlinear effects, which requires the engineer to make decisions about the required modeling effort and associated computational time to achieve a desired level of accuracy. For steel frames modeled with beam elements, these nonlinear effects are accounted for using a geometric stiffness matrix and a solution scheme that incrementally applies the load(s) to closely approximate the 'exact' equilibrium of the frame in the deformed configuration. The accuracy in modeling the frame in this configuration is dependent upon the number of elements that are used to model each member and on the number of load increments that are used to apply the external load(s). Increasing the number of elements per member and the number of load increments to improve accuracy often comes at a cost of increased computational time since buildings have a large number of load combinations that need to be considered. This paper presents and assesses the performance of a new geometric stiffness matrix to potentially reduce the required number of elements per member and the required number of load increments to achieve a specified level of accuracy. The effects

[1] Graduate Student, Florida Atlantic University, <nfaramawi2019@fau.edu>
[2] Professor, Florida Atlantic University, <rosson@fau.edu>

of nonlinear material behavior are not considered in this study as the majority of routine building design considers only linear, elastic material behavior (Ziemian and Ziemian 2021).

Assessment of the new geometric stiffness matrix is conducted on two columns and five frames with known 'exact' closed-form solutions (Galambos and Surovek 2008). The number of load increments to achieve a one percent relative error is evaluated on four unbraced frames with an initial geometric imperfection of H/500. Based on these results, the paper uses the amplification factor based on the second-order results compared with the first-order results to explore the minimum number of load increments needed to achieve this level of accuracy. To assist the engineer in selecting the number of load increments to use for a given frame and loading condition, the frame's elastic buckling load factor $\alpha_{cr}$ is used to approximate the amplification factor $AF_{\alpha_{cr}}$ (Merchant 1954, Eurocode EN 1993-1-1 2005, and AS 4100 2020). A single increment predictor-corrector (SIPC) solution scheme was studied by Ziemian and Ziemian (2021) as an approximate second-order elastic analysis method for routine design of steel and aluminum frames. Their study of 22 benchmark frames revealed an error range of 0.65% to 5.50% for frames with $\alpha_{cr} \geq 3$.

All frames were modeled using the MASTAN2 (2014) analysis software, which accounts for second-order effects using an Updated Lagrangian formulation, and for this study, the predictor-corrector solution scheme. The software is also capable of performing a linear buckling analysis (LBA) using the inverse iteration method (McGuire *et al*. 2000). All members were modeled as planar 6-dof line elements with elastic material behavior. Models have perfect geometries when comparing the results with the 'exact' solutions, and they have out-of-plumb geometries when performing the nonlinear analyses of the four unbraced frames and 22 benchmark frames.

**2. New Geometric Stiffness Matrix**

A nonlinear tangent stiffness matrix for a beam-column element was developed by Ekhande *et al*. (1989) using stability functions to account for the effect of axial force on flexural stiffness. The explicit expressions for the stability functions of a planar beam-column are given in Eqs. 1 – 5.

$$\beta = L\sqrt{\frac{P}{EI}} \tag{1}$$

$$C_1 = \frac{\beta^2(1-cos\beta)}{2sin\beta\left(tan\frac{\beta}{2}-\frac{\beta}{2}\right)} \tag{2}$$

$$C_2 = \frac{\beta(sin\beta-\beta cos\beta)}{2sin\beta\left(tan\frac{\beta}{2}-\frac{\beta}{2}\right)} \tag{3}$$

$$C_3 = \frac{\beta(\beta-sin\beta)}{2sin\beta\left(tan\frac{\beta}{2}-\frac{\beta}{2}\right)} \tag{4}$$

$$C_4 = \frac{\beta^3 sin\beta}{2sin\beta\left(tan\frac{\beta}{2}-\frac{\beta}{2}\right)} \tag{5}$$

Using the geometric stiffness matrix as developed by Yang and McGuire (1986) for use in an Updated Lagrangian nonlinear elastic analysis, the stability functions appear in the global stiffness matrix for a planar beam element as given in Eqs. 6 – 9.

$$\boldsymbol{R}^T\left[\boldsymbol{K}_e + \boldsymbol{K}_g\right]\boldsymbol{R} = \begin{bmatrix} \boldsymbol{K}_{11} & \boldsymbol{K}_{12} \\ \boldsymbol{K}_{21} & \boldsymbol{K}_{22} \end{bmatrix} \tag{6}$$

$$\boldsymbol{K}_{11} = \begin{bmatrix} \frac{EA}{L}cos^2\theta + C_4\frac{EI}{L^3}sin^2\theta & \left(\frac{EA}{L} - C_4\frac{EI}{L^3}\right)cos\theta sin\theta & -C_1\frac{EI}{L^2}sin\theta \\ \left(\frac{EA}{L} - C_4\frac{EI}{L^3}\right)cos\theta sin\theta & \frac{EA}{L}sin^2\theta + C_4\frac{EI}{L^3}cos^2\theta & C_1\frac{EI}{L^2}cos\theta \\ -C_1\frac{EI}{L^2}sin\theta & C_1\frac{EI}{L^2}cos\theta & C_2\frac{EI}{L} \end{bmatrix} \tag{7}$$

$$\boldsymbol{K}_{12} = \boldsymbol{K}_{21} = \begin{bmatrix} -\frac{EA}{L}cos^2\theta - C_4\frac{EI}{L^3}sin^2\theta & -\left(\frac{EA}{L} - C_4\frac{EI}{L^3}\right)cos\theta sin\theta & -C_1\frac{EI}{L^2}sin\theta \\ -\left(\frac{EA}{L} - C_4\frac{EI}{L^3}\right)cos\theta sin\theta & -\frac{EA}{L}sin^2\theta - C_4\frac{EI}{L^3}cos^2\theta & C_1\frac{EI}{L^2}cos\theta \\ C_1\frac{EI}{L^2}sin\theta & -C_1\frac{EI}{L^2}cos\theta & C_3\frac{EI}{L} \end{bmatrix} \tag{8}$$

$$\boldsymbol{K}_{22} = \begin{bmatrix} \frac{EA}{L}cos^2\theta + C_4\frac{EI}{L^3}sin^2\theta & \left(\frac{EA}{L} - C_4\frac{EI}{L^3}\right)cos\theta sin\theta & C_1\frac{EI}{L^2}sin\theta \\ \left(\frac{EA}{L} - C_4\frac{EI}{L^3}\right)cos\theta sin\theta & \frac{EA}{L}sin^2\theta + C_4\frac{EI}{L^3}cos^2\theta & -C_1\frac{EI}{L^2}cos\theta \\ C_1\frac{EI}{L^2}sin\theta & -C_1\frac{EI}{L^2}cos\theta & C_2\frac{EI}{L} \end{bmatrix} \tag{9}$$

Yang and McGuire (1986) presented simplified 2nd-order expressions for the stability functions in their geometrical stiffness matrix [$k_g$] as given in Eqs. 10 – 13. These equations have been used extensively over the decades and are included in the source code of MASTAN2 (2014).

$$C_1 = 6 - \frac{\beta^2}{10} \tag{10}$$

$$C_2 = 4 - \frac{2\beta^2}{15} \tag{11}$$

$$C_3 = 2 + \frac{\beta^2}{30} \tag{12}$$

$$C_4 = 12 - \frac{6\beta^2}{5} \tag{13}$$

These simplified 2nd-order expressions begin to deviate from the 'exact' expressions when $\beta > 2$ as illustrated in Fig. 1. In order to reduce this error, while maintaining the simplicity and numerical

stability of a 6th-order polynomial expression, Eqs. 14 – 17 were developed based on a nonlinear regression analysis of data produced using $\beta$ increments of 0.01 ($r^2$ = 0.999) in Eqs. 2 – 5.

$$C_1 = 6 - \frac{1{,}031\beta^2}{10{,}000} - \frac{227\beta^6}{5{,}000{,}000} \tag{14}$$

$$C_2 = 4 - \frac{1{,}403\beta^2}{10{,}000} - \frac{733\beta^6}{5{,}000{,}000} \tag{15}$$

$$C_3 = 2 + \frac{743\beta^2}{20{,}000} + \frac{2\beta^6}{19{,}763} \tag{16}$$

$$C_4 = 12 - \frac{603\beta^2}{500} - \frac{466\beta^6}{5{,}128{,}205} \tag{17}$$

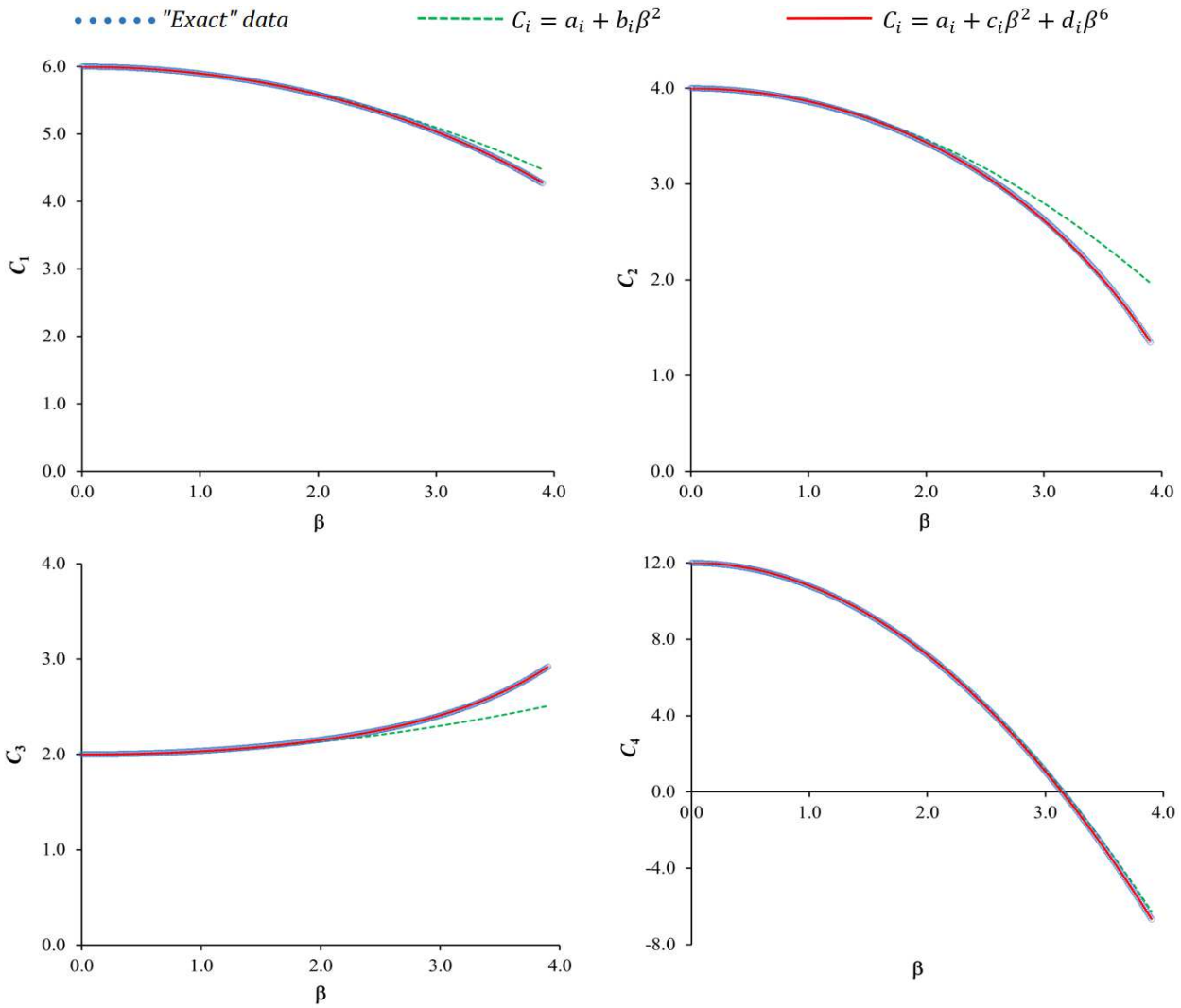


Figure 1: 2nd-order and 6th-order polynomial approximations for $C_1$, $C_2$, $C_3$ and $C_4$

## 3. Braced Columns and Frames

The potential benefit of using the 6th-order polynomial expressions was studied by considering two braced columns and two braced frames with known critical buckling load equations (Galambos and Surovek 2008). The columns and frames in Fig. 2 were used to determine if the number of elements per member that are needed to accurately determine the critical buckling load can be reduced by using the new expressions. Eqs. 10 – 13 are already in MASTAN2, and Eqs. 14 – 17 were added to the source code. MASTAN2 uses the inverse iteration method to determine the minimum eigenvalue or critical load ratio (McGuire *et al*. 2000). In this method, the geometric stiffness matrix $\mathbf{K_{g,ff}}$ is evaluated only once and is dependent upon the magnitude of the initial input load $P_{ref}$. All structures in this study are evaluated with $E = I = L = 1$, unless stated otherwise.

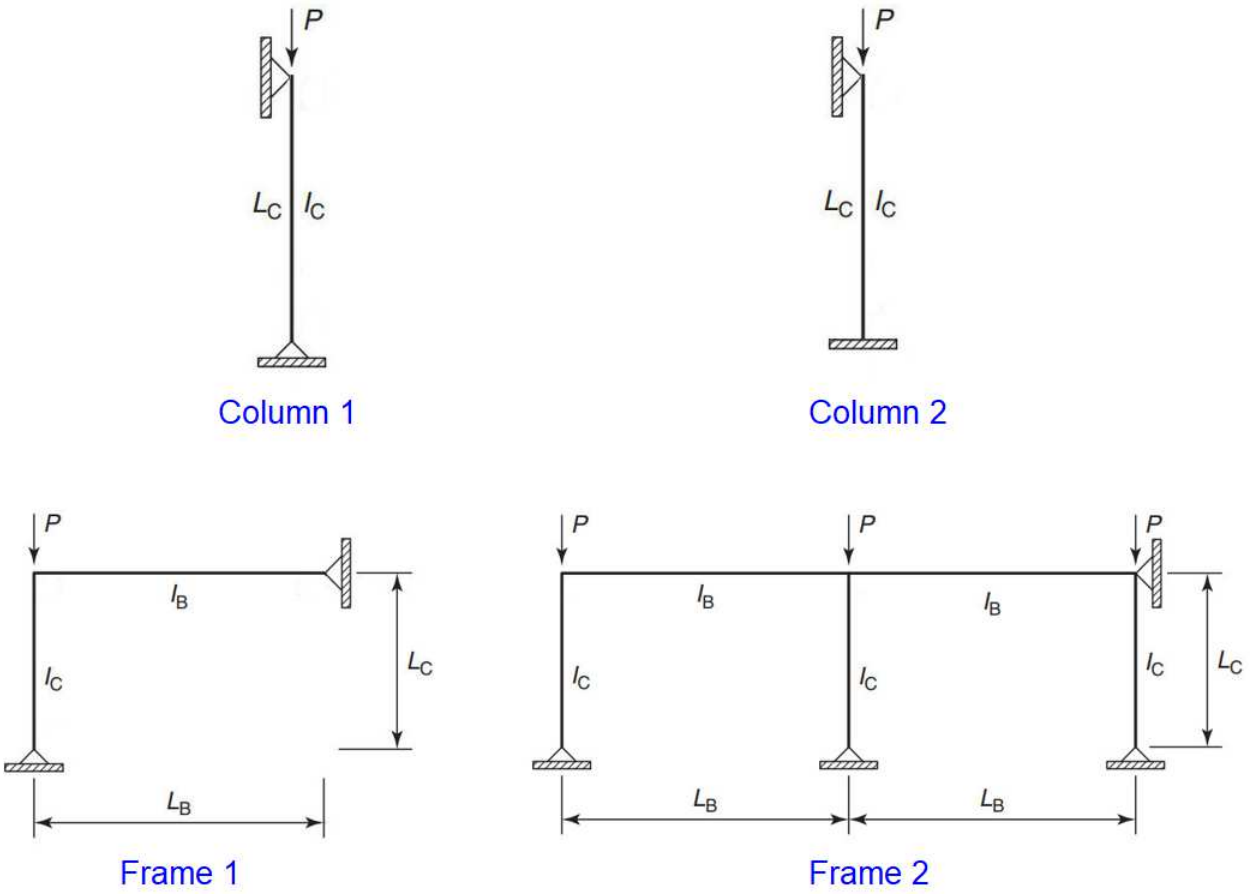


Figure 2: Braced columns and frames

The relative error is used to evaluate each modeled condition as given in Eq. 18 where $P$ is determined from closed-form equations (Galambos and Surovek 2008), and $P_{cr}$ is determined from a 2nd-Order Elastic analysis in MASTAN2. Using the original $\mathbf{K_g}$ and the new $\mathbf{K_g}$ in MASTAN2, Column 1 in Fig. 2 has $\beta = \pi$ in Eq. 19, and $P = \pi^2$ in Eq. 1.

$$\text{Rel. Error} = \frac{P_{cr} - P}{P} \cdot 100\% \tag{18}$$

$$sin\beta = 0 \tag{19}$$

As given in Table 1, high relative errors are produced with $P_{ref}$ = 1 when using only one element to model the column, but the new expressions give a relative error of less than one percent when using only one element when $P_{ref} \approx P$. The old expressions give good results when two or more elements are used, and there is no $P_{ref}$ effect when four elements are used.

Table 1: Column 1 analysis conditions and results

| | | **Original $K_g$** | | | | **New $K_g$** | | | |
|---|---|---|---|---|---|---|---|---|---|
| $P_{ref}$ | Elem/Mem | ALR | $P_{cr}$ | K | Rel. Error | ALR | $P_{cr}$ | K | Rel. Error |
| 1 | 1 | 12.00 | 12.00 | 0.907 | 21.59 | 11.26 | 11.26 | 0.936 | 14.09 |
| 9.87 | 1 | 1.216 | 12.00 | 0.907 | 21.59 | 1.005 | 9.921 | 0.997 | 0.52 |
| 9.87 | 2 | 1.008 | 9.944 | 0.996 | 0.75 | 0.995 | 9.820 | 1.003 | -0.50 |
| 9.87 | 4 | 1.001 | 9.875 | 1.000 | 0.05 | 0.997 | 9.844 | 1.001 | -0.26 |
| 1 | 4 | 9.875 | 9.875 | 1.000 | 0.05 | 9.844 | 9.844 | 1.001 | -0.26 |

Column 2 in Fig. 2 has $\beta$ = 4.49341 in Eq. 20, and $P$ = 20.1907 in Eq. 1.

$$tan\beta - \beta = 0 \tag{20}$$

As indicated in Table 2, high relative errors are produced with $P_{ref}$ = 1 when only one element is used, but the new expressions give a relative error of less than one percent when using only one element when $P_{ref} \approx P$. The old expressions give comparable results only when four elements are used to model the column.

Table 2: Column 2 analysis conditions and results

| | | **Original $K_g$** | | | | **New $K_g$** | | | |
|---|---|---|---|---|---|---|---|---|---|
| $P_{ref}$ | Elem/Mem | ALR | $P_{cr}$ | K | Rel. Error | ALR | $P_{cr}$ | K | Rel. Error |
| 1 | 1 | 30.00 | 30.00 | 0.574 | 48.59 | 28.48 | 28.48 | 0.589 | 41.06 |
| 20.19 | 1 | 1.485 | 30.00 | 0.574 | 48.59 | 0.990 | 19.99 | 0.703 | -0.99 |
| 20.19 | 2 | 1.025 | 20.71 | 0.690 | 2.58 | 0.998 | 20.15 | 0.700 | -0.20 |
| 20.19 | 4 | 1.002 | 20.23 | 0.698 | 0.20 | 0.995 | 20.11 | 0.701 | -0.40 |
| 1 | 4 | 20.23 | 20.23 | 0.698 | 0.20 | 20.11 | 20.11 | 0.701 | -0.40 |

Frame 1 in Fig. 2 is used to study the effect of differing column and beam stiffnesses on the modeling results. The $\gamma$ = 4.6, 8 and 24 conditions in Table 3 produce $\beta$ = 4.2152, 4.32205 and 4.43275 in Eq. 22, and $P$ = 17.7679, 18.6801 and 19.6493 in Eq. 1, respectively.

$$\gamma = \frac{I_B L_C}{I_C L_B} \tag{21}$$

$$tan\beta - \frac{3\gamma\beta}{\beta^2 + 3\gamma} = 0 \tag{22}$$

The new expressions give good results when using one element per member with $P_{ref} \approx P$, but four elements per member are needed with the old expressions to give comparable results to those with the new expressions. As with the two columns, high relative errors occur with $P_{ref} = 1$ when using only one element per member.

Table 3: Frame 1 analysis conditions and results

| | | | **Original $K_g$** | | | | **New $K_g$** | | | |
|---|---|---|---|---|---|---|---|---|---|---|
| $P_{ref}$ | $\gamma$ | Elem/Mem | ALR | $P_{cr}$ | K | Rel. Error | ALR | $P_{cr}$ | K | Rel. Error |
| 1 | 4.6 | 1 | 25.71 | 25.64 | 0.620 | 44.31 | 24.27 | 24.21 | 0.638 | 36.26 |
| 17.77 | 4.6 | 1 | 1.447 | 25.64 | 0.620 | 44.31 | 0.991 | 17.56 | 0.750 | -1.17 |
| 17.77 | 4.6 | 4 | 1.001 | 17.74 | 0.746 | -0.16 | 0.996 | 17.65 | 0.748 | -0.66 |
| 18.68 | 8 | 1 | 1.464 | 27.27 | 0.602 | 45.99 | 0.990 | 18.44 | 0.732 | -1.28 |
| 19.65 | 24 | 1 | 1.478 | 28.95 | 0.584 | 47.33 | 0.989 | 19.37 | 0.714 | -1.42 |

Frame 2 in Fig. 2 is used to study the effect of the number of elements per member on the relative error. The $\gamma = 2/3$ condition in Table 4 gives $\beta = 3.53992$ in Eq. 24, and $P = 12.5310$ in Eq. 1.

$$c = \frac{1}{\beta^2}\left(1 - \frac{\beta}{tan\beta}\right) \tag{23}$$

$$\left(\frac{1}{c^2} + \frac{12\gamma}{c} + 24\gamma^2\right) = 0 \tag{24}$$

As with the two columns, high relative errors occur with $P_{ref} = 1$ when using only one element per member, but there is no $P_{ref}$ effect when four elements per member are used. The new expressions give a relative error of less than one percent when using only one element when $P_{ref} \approx P$, but two or more elements are needed to obtain comparable errors with the old expressions.

Table 4: Frame 2 analysis conditions and results

| | | | **Original $K_g$** | | | | **New $K_g$** | | | |
|---|---|---|---|---|---|---|---|---|---|---|
| $P_{ref}$ | $\gamma$ | Elem/Mem | ALR | $P_{cr}$ | K | Rel. Error | ALR | $P_{cr}$ | K | Rel. Error |
| 1 | 0.667 | 1 | 16.24 | 16.24 | 0.780 | 29.61 | 15.24 | 15.24 | 0.805 | 21.63 |
| 12.53 | 0.667 | 1 | 1.296 | 16.24 | 0.780 | 29.61 | 1.001 | 12.54 | 0.887 | 0.08 |
| 12.53 | 0.667 | 2 | 1.009 | 12.64 | 0.884 | 0.88 | 0.996 | 12.48 | 0.889 | -0.38 |
| 12.53 | 0.667 | 4 | 1.000 | 12.53 | 0.888 | 0.00 | 0.997 | 12.49 | 0.889 | -0.28 |
| 1 | 0.667 | 4 | 12.53 | 12.53 | 0.888 | 0.00 | 11.89 | 12.49 | 0.889 | -0.28 |

## 4. Unbraced Frames

The new 6th-order polynomial expressions were also studied using three unbraced frames with known critical buckling load equations (Galambos and Surovek 2008) and one unbraced frame that was analyzed with a step size of 0.001 in a second-order elastic analysis using a predictor-corrector solution scheme. The first three unbraced frames in Fig. 3 were used to investigate the $P_{ref}$ requirements and the number of elements per member that are needed to achieve accurate critical buckling load results. The number of load increments that are needed to obtain results with a relative error of one percent or less was also studied with all four unbraced frames.

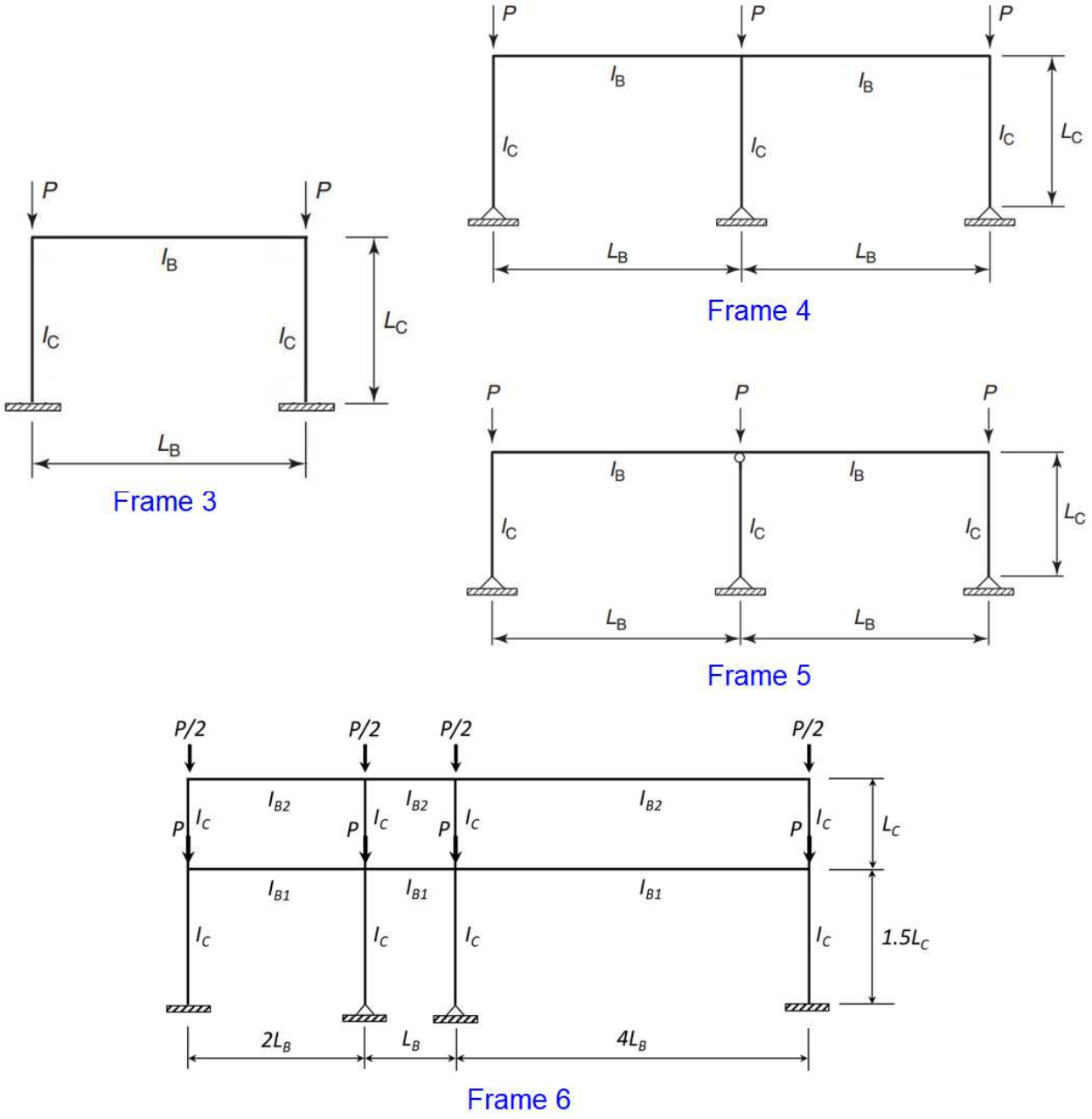


Figure 3: Unbraced frames

Frame 3 in Fig. 3 is used to study the $P_{ref}$ effect and the number of elements per member on the relative error. The $\gamma$ = 2/3, 1, 2, 8 and 24 conditions in Table 5 produce $\beta$ = 2.5705, 2.7165, 2.9042, 3.0774 and 3.1200 in Eq. 25, and $P$ = 6.6075, 7.3794, 8.4343, 9.4704 and 9.7344 in Eq. 1, respectively.

$$\frac{tan\beta}{\beta} + \frac{1}{6\gamma} = 0 \tag{25}$$

In Table 5 it is noticed that even with only one element per member and $P_{ref}$ = 1, the relative errors are all very small when using either the old or new polynomial expressions in **$K_g$**. For this unbraced frame, with its wide range of beam and column stiffness conditions, it is sufficient to use only one element per member to accurately determine the critical buckling load.

Table 5: Analysis conditions and results for Frame 3

| | | | **Original $K_g$** | | | | **New $K_g$** | | | |
|---|---|---|---|---|---|---|---|---|---|---|
| $P_{ref}$ | $\gamma$ | Elem/Mem | ALR | $P_{cr}$ | K | Rel. Error | ALR | $P_{cr}$ | K | Rel. Error |
| 1 | 0.667 | 1 | 6.635 | 6.635 | 1.220 | 0.42 | 6.603 | 6.603 | 1.223 | -0.07 |
| 1 | 1 | 1 | 7.401 | 7.401 | 1.155 | 0.29 | 7.369 | 7.369 | 1.157 | -0.14 |
| 1 | 2 | 1 | 8.454 | 8.454 | 1.080 | 0.23 | 8.419 | 8.419 | 1.083 | -0.18 |
| 1 | 8 | 1 | 9.505 | 9.505 | 1.019 | 0.37 | 9.461 | 9.461 | 1.021 | -0.10 |
| 1 | 24 | 1 | 9.776 | 9.776 | 1.005 | 0.43 | 9.729 | 9.729 | 1.007 | -0.06 |

Numerous second-order elastic analyses were conducted to determine the minimum number of load increments that were needed to limit the relative error to one percent or less. Frames 3, 4, and 5 were modeled with an initial geometric imperfection of H/500 and an increment size of 0.001 in a predictor-corrector solution scheme to obtain the 'exact' results. The $\gamma$ = 1, 8, and 24 conditions were used with six different P load magnitudes for each $\gamma$ condition. The amplification factor was evaluated for each analysis condition using Eq. 26, where $\Delta_{2nd}$ is the lateral displacement of the top left node of the frame from a second-order elastic analysis, and $\Delta_{1st}$ is the displacement at the same location from a first-order elastic analysis.

$$AF = \frac{\Delta_{2nd}}{\Delta_{1st}} \tag{26}$$

As indicated in Fig. 4, a linear relationship exists between the minimum number of load increments that are needed to keep the relative error below one percent and the amplification factor.

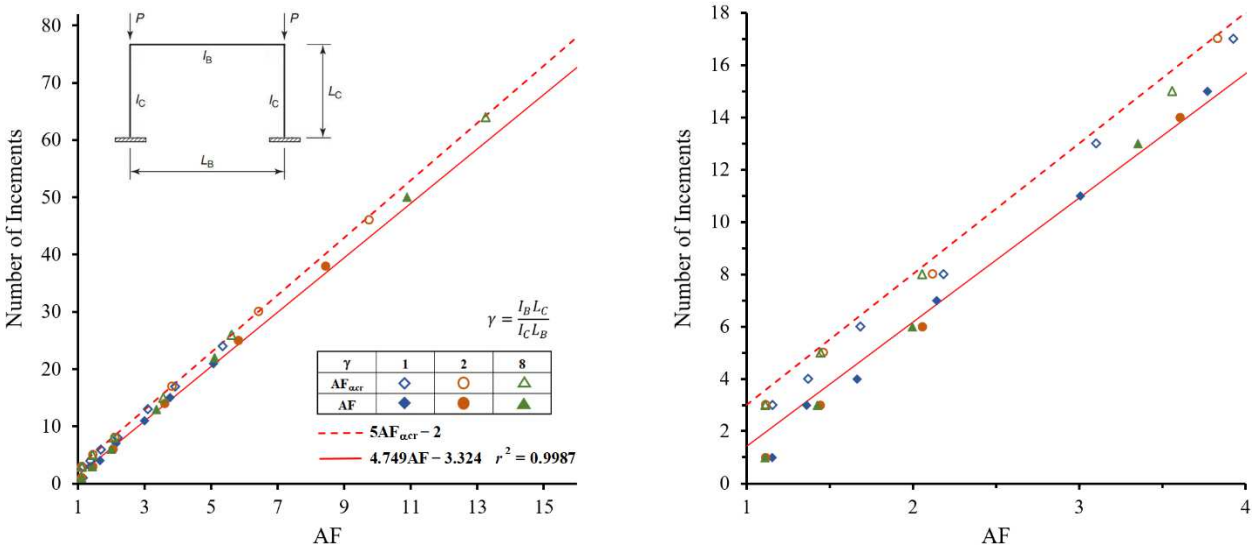

Figure 4: Number of increments vs. amplification factor for Frame 3 (relative error ≤ 1%)

A regression analysis of the data revealed a very strong linear relationship (red line, $r^2$ = 0.9987). With a slope of approximately 5 and *y*-intercept of approximately 3, Eq. 27 is proposed for design purposes to determine the minimum number of load increments to use in a second-order elastic analysis with the predictor-corrector solution scheme. It conservatively uses 2 for the *y*-intercept because only the integer is used from the calculation result, and it also ensures the relative errors remain below one percent.

$$\text{Number of Increments} = 5AF_{\alpha_{cr}} - 2 \tag{27}$$

$AF_{\alpha_{cr}}$ is the approximate amplification factor which is based on the elastic buckling load ratio of the frame $\alpha_{cr}$ as given in Eurocode EN 1993-1-1 (2005) and AS 4100 (2020). The critical buckling load $P_{cr}$ in Eq. 29 is obtained from Table 5, and P is the applied load on the frame.

$$AF_{\alpha_{cr}} = \frac{1}{1 - 1/\alpha_{cr}} \tag{28}$$

$$\alpha_{cr} = \frac{P_{cr}}{P} \tag{29}$$

As indicated by the dashed red line in Fig. 4, and the corresponding data associated with it, the minimum number of load increments as determined from Eq. 27 was found to produce second-order elastic results that were within one percent of the 'exact' results.

Frame 4 in Fig. 3 is used to study the $P_{ref}$ effect and the number of elements per member on the relative error. The $\gamma$ = 2/3 condition in Table 6 produces $\beta$ = 1.29913 in Eq. 30, and $P$ = 1.6877 in Eq. 1. As before with Frame 3, when using only one element per member and $P_{ref}$ = 1, the relative errors are very small when using either the old or new polynomial expressions in $\mathbf{K_g}$. There is also little beneficial effect when using more elements per member or when $P_{ref} \approx P$.

$$\beta^2\left(\frac{1}{c^2} + \frac{12\gamma}{c} + 24\gamma^2\right) - \frac{8\gamma}{c}\left(\frac{1}{c} + 3\gamma\right) = 0 \tag{30}$$

Table 6: Analysis conditions and results for Frame 4

| | | | **Original $K_g$** | | | | **New $K_g$** | | | |
|---|---|---|---|---|---|---|---|---|---|---|
| $P_{ref}$ | $\gamma$ | Elem/Mem | ALR | $P_{cr}$ | K | Rel. Error | ALR | $P_{cr}$ | K | Rel. Error |
| 1 | 0.667 | 1 | 1.691 | 1.691 | 2.416 | 0.20 | 1.691 | 1.691 | 2.416 | 0.20 |
| 1.688 | 0.667 | 1 | 1.002 | 1.691 | 2.416 | 0.20 | 0.997 | 1.682 | 2.422 | -0.34 |
| 1.688 | 0.667 | 2 | 1.000 | 1.687 | 2.419 | -0.04 | 0.998 | 1.685 | 2.420 | -0.16 |
| 1.688 | 0.667 | 4 | 1.000 | 1.687 | 2.419 | -0.04 | 0.999 | 1.687 | 2.419 | -0.04 |
| 1 | 0.667 | 4 | 1.687 | 1.687 | 2.419 | -0.04 | 1.687 | 1.687 | 2.419 | -0.04 |

As indicated in Fig. 5 with Frame 4, a linear relationship also exists between the minimum number of load increments and the amplification factor. A regression analysis of the data revealed a linear relationship (red line, $r^2$ = 0.9994) with approximately the same slope and *y*-intercept as that given

in Fig. 4 with Frame 3. As before, Eq. 27 was found to produce second-order elastic results for Frame 4 that were within one percent of the 'exact' results.

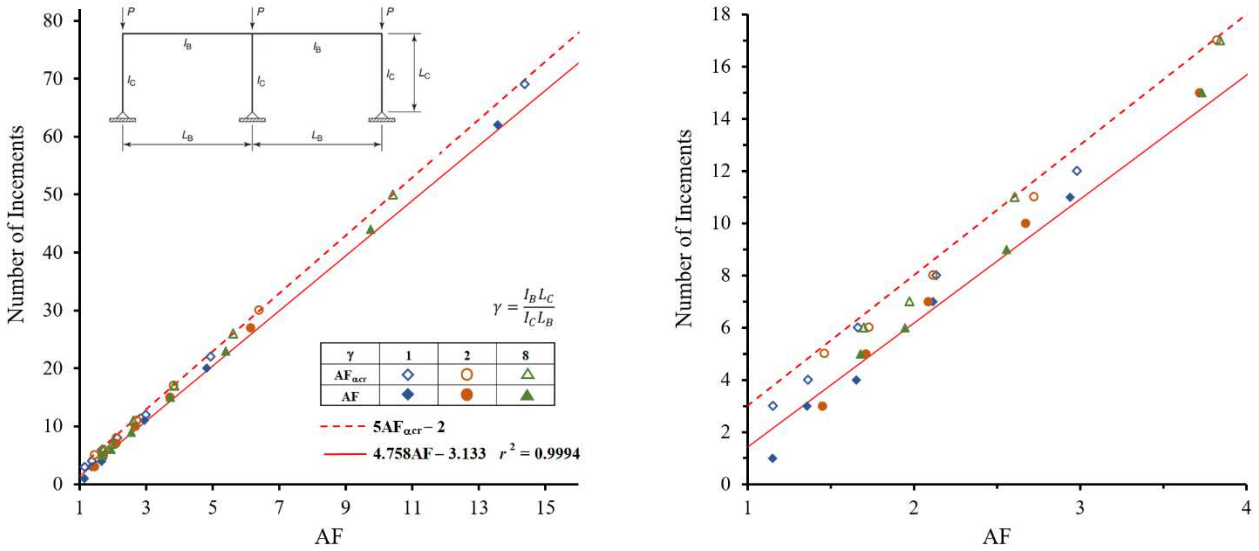


Figure 5: Number of increments vs. amplification factor for Frame 4 (relative error ≤ 1%)

Frame 5 in Fig. 3 is very similar to Frame 4, the only difference is the internal hinge at the top of the middle column. This frame was used to determine if this had any effect on the use of Eq. 27 to determine the minimum number of load increments and on the modeling conditions to obtain an accurate $P_{cr}$. The $\gamma = 2$ condition in Table 7 produces $\beta = 1.11978$ in Eq. 31, and $P = 1.2539$ in Eq. 1. As before with Frames 3 and 4, when using only one element per member, the relative errors are very small when using either the old or new polynomial expressions in $\mathbf{K_g}$. There is also little beneficial effect when using more elements per member or when $P_{ref} \approx P$.

$$3\beta^2\left(\frac{2}{c} + 6\gamma\right) - \frac{12\gamma}{c} = 0 \tag{31}$$

Table 7: Analysis conditions and results for Frame 5

| | | | **Original $\mathbf{K_g}$** | | | | **New $\mathbf{K_g}$** | | | |
|---|---|---|---|---|---|---|---|---|---|---|
| $P_{ref}$ | γ | Elem/Mem | ALR | $P_{cr}$ | K | Rel. Error | ALR | $P_{cr}$ | K | Rel. Error |
| 1 | 2 | 1 | 1.255 | 1.255 | 2.804 | 0.08 | 1.250 | 1.250 | 2.810 | -0.32 |
| 1.254 | 2 | 1 | 1.001 | 1.255 | 2.804 | 0.08 | 0.997 | 1.250 | 2.810 | -0.32 |
| 1.254 | 2 | 2 | 0.999 | 1.253 | 2.807 | -0.08 | 0.998 | 1.252 | 2.808 | -0.16 |
| 1.254 | 2 | 4 | 0.999 | 1.253 | 2.807 | -0.08 | 0.999 | 1.253 | 2.807 | -0.08 |
| 1 | 2 | 4 | 1.253 | 1.253 | 2.807 | -0.08 | 1.253 | 1.253 | 2.807 | -0.08 |

As indicated in Fig. 6 with Frame 5, a similar linear relationship exists between the minimum number of load increments and the amplification factor. The internal hinge has no effect on the use of Eq. 27 to determine the minimum number of load increments since it was found to produce second-order elastic results for Frame 5 that were within one percent of the 'exact' results.

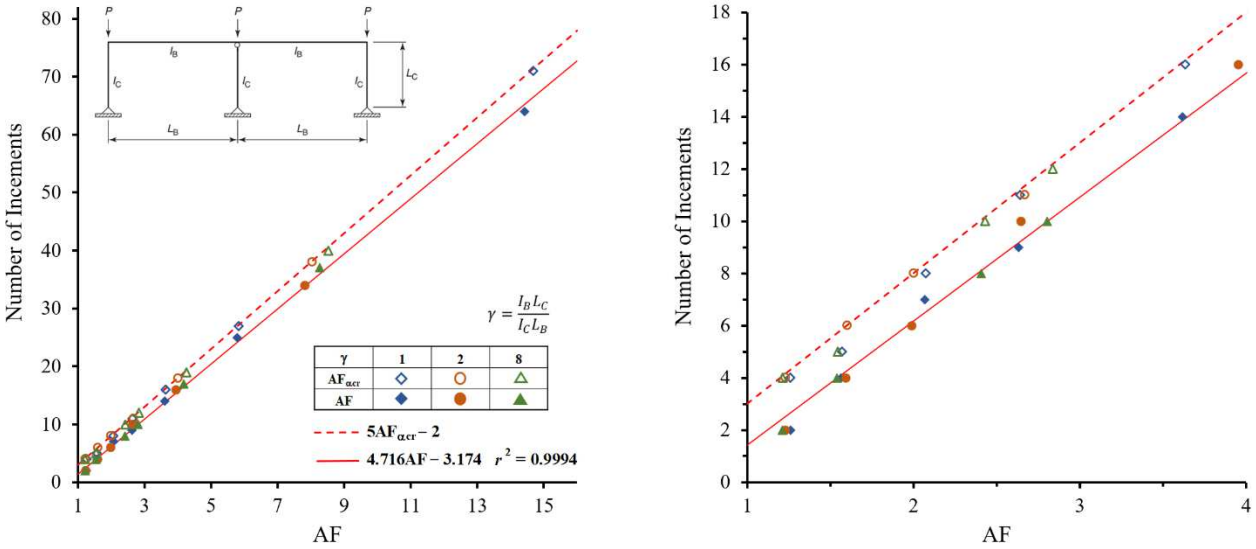


Figure 6: Number of increments vs. amplification factor for Frame 5 (relative error ≤ 1%)

Frame 6 in Fig. 3 was developed to evaluate the effectiveness of Eq. 27 on a more complex unbraced frame. A linear buckling analysis was conducted using MASTAN2 on six different beam and column stiffness configurations as given in Table 8. Configurations A, D, and F were used to conduct second-order elastic analyses with six magnitudes of external load for each configuration.

$$\gamma_1 = \frac{I_{B1} L_C}{I_C L_B} \tag{32}$$

$$\gamma_2 = \frac{I_{B2} L_C}{I_C L_B} \tag{33}$$

Table 8: Analysis conditions and results for Frame 6

| Configuration | $\gamma_1$ | $\gamma_2$ | $P_{cr}$ |
|---|---|---|---|
| A | 1 | 2 | 1.352 |
| B | 8 | 2 | 1.677 |
| C | 24 | 2 | 1.768 |
| D | 0.5 | 1 | 2.406 |
| E | 4 | 1 | 3.160 |
| F | 12 | 1 | 3.426 |

As indicated in Fig. 7, Frame 6 also has a linear relationship between the minimum number of load increments and the amplification factor. A regression analysis of the data revealed a similar linear relationship (red line, $r^2 = 0.9991$) with approximately the same slope and *y*-intercept as those for Frames 3, 4, and 5. As with the previous unbraced frames, Eq. 27 was found to produce second-order elastic results for Frame 6 that were within one percent of the 'exact' results.

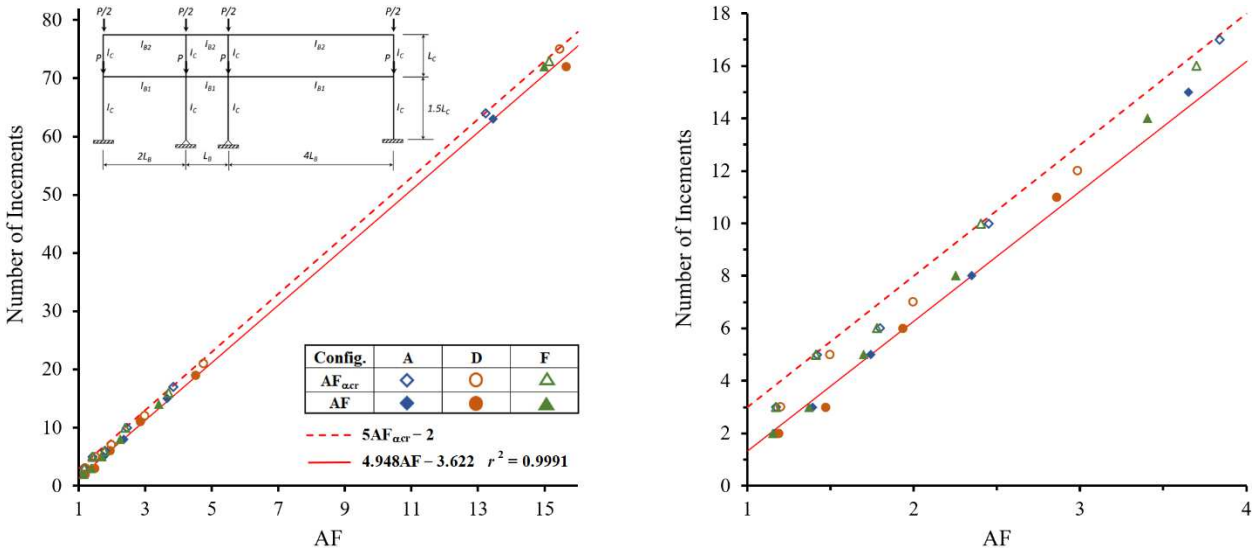


Figure 7: Number of increments vs. amplification factor for Frame 6 (relative error ≤ 1%)

## 5. Validation Study with 22 Benchmark Frames

With successful applications of Eq. 27 in the previous section, the 22 benchmark frames studied by Ziemian and Ziemian (2021) were used to further test the validity of the expression to determine the minimum number of load increments in a second-order elastic analysis using the predictor-corrector solution scheme. The 22 frames of the validation study are given in Table 9. All of the section properties, material properties, modeling conditions, and loads are the same as those used in their study. The 'exact' results that were obtained by using an incremental-iterative work control scheme with 1,000 load increments. As indicated in Fig. 8, a similar linear relationship exists between the minimum number of load increments and the amplification factor. Eq. 27 was found to produce results for all 22 frames that were within one percent of the 'exact' results, thus demonstrating the validity of this simple equation to accurately and efficiently conduct second-order analyses when designing steel frames.

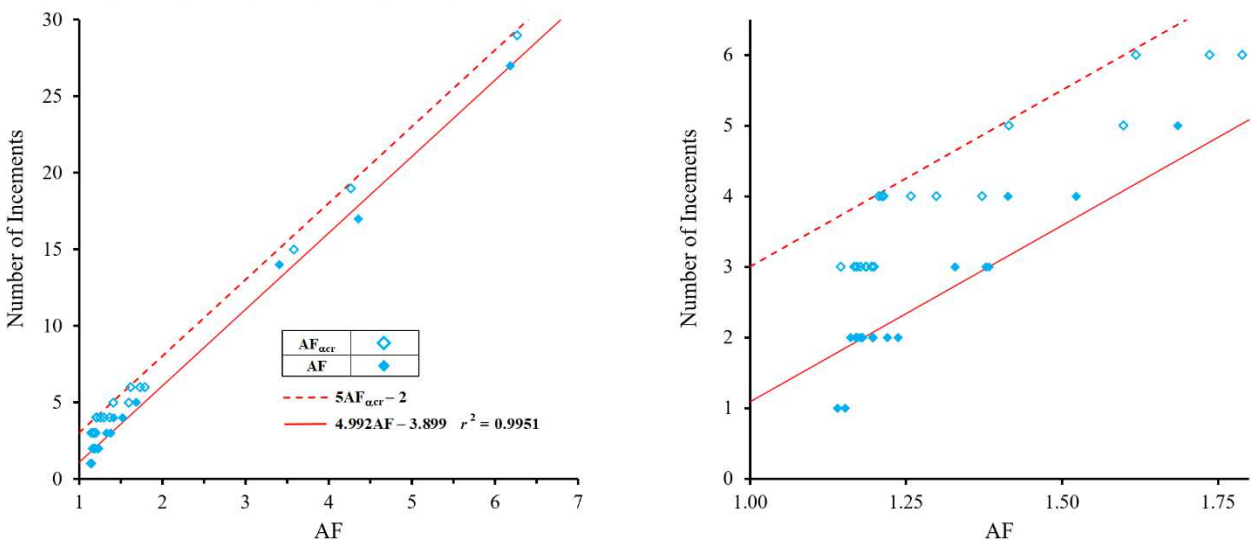


Figure 8: Number of increments vs. amplification factor for 22 benchmark frames (relative error ≤ 1%)

| Frame No. | Description | Geometry | Load Combination | Frame No. | Description | Geometry | Load Combination |
|---|---|---|---|---|---|---|---|
| 1 | 1 story, 1 bay [Ziemian 1990] |  | 1.2D + 1.6L$_r$ + 0.5W | 11 | 2 stories, 1 bay & 3 stories 1 bay [Schimizze 2001] |  | 1.2D + 1.0L + 0.5L$_r$ +1.0W |
| 2 | Gable; 1 story, 1 bay [Schimizze 2001] |  | 1.2D + 0.5L$_r$ + 1.0W | 12 | 6 stories, 2 bays [Vogel 1985] |  | 1.2D + 1.0L + 0.5L$_r$ +1.0W |
| 3 | 2 stories, 1 bay [Deierlein et al. 2002] |  | 1.2D + 1.0L + 1.0W | 13-16 | 10 stories, 3 bays; 0, 4, 8, 12 lean-ons [Lu et al. 1977; Statler et al. 2011] | 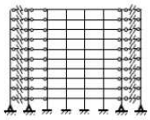 | 1.2D + 1.0L + 0.5L$_r$ +1.0W |
| 4 | 1 story, 1 bay (10 lean-on) [Maleck 2001] | 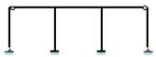 | 1.2D+1.6Lr | | | | |
| 5 | 1 story, 2 bays [Martinez-Garcia et al. 2006] | 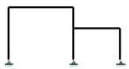 | 1.2D + 1.6L$_r$ + 0.5W | 17 | 10 stories, 5 bays [Lu et al. 1977] | | 1.2D + 1.0L + 0.5L$_r$ +1.0W |
| 6 | 1 story, 2 bays [Martinez-Garcia et al. 2006] | 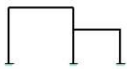 | 1.2D + 1.6L$_r$ + 0.5W | 18 | 20 stories, 1 bay [Lu et al. 1977] | | 1.2D + 1.0L + 0.5L$_r$ +1.0W |
| 7 | 1 story, 1 bay braced, with lean-on [Martinez-Garcia et al. 2006] | 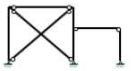 | 1.2D + 1.6L$_r$ + 0.5W | 19 | 26 stories, 3 bays [Lu et al. 1977] | 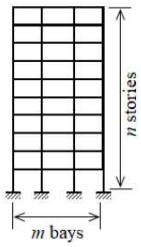 | 1.2D + 1.0L + 0.5L$_r$ +1.0W |
| 8 | 1 story, 1 bay braced, with lean-on (minor axis) [Martinez-Garcia et al. 2006] | 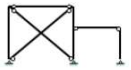 | 1.2D + 1.6L$_r$ + 0.5W | 20 | 30 stories, 2 bays [Lu et al. 1977] | | 1.2D + 1.0L + 0.5L$_r$ +1.0W |
| 9 | 2 stories, 2 bays [Iffland et al. 1982; Ziemian et al. 1992] | 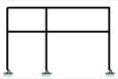 | 1.2D + 1.6L + 0.5L$_r$ | 21 | 30 stories, 2 bays [Lu et al. 1977] | | 1.2D + 1.0L + 0.5L$_r$ +1.0W |
| 10 | 2 stories, 2 bays (minor axis) [Ziemian & Miller 1997] | 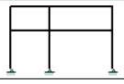 | 1.2D + 1.6L + 0.5L$_r$ | 22 | 40 stories, 2 bays [Lu et al. 1977] | | 1.2D + 1.0L + 0.5L$_r$ +1.0W |

Table 9: Overview of 22 benchmark frames (Ziemian & Ziemian 2021)

## 6. Conclusions

This paper presented a new geometric stiffness matrix with 6$^{th}$-order polynomial expressions for the coefficients that more closely approximate the theoretically derived stability functions. It was found that the new geometric stiffness matrix gave improved results only when the structures were braced and when $P_{ref}$ was close to the critical buckling load. Under these conditions, it was found that only one element per member was needed to obtain excellent results, and this held true over a wide range of beam-to-column stiffness ratios of braced frames. The critical buckling load studies of unbraced frames revealed there was little to no advantage to using the new 6$^{th}$-order expressions.

Based on the displacement results of the four unbraced frames and 22 benchmark frames, a linear relationship was discovered between the amplification factor and the minimum number of load increments that are needed to limit the relative error to one percent. The integer result of $5AF_{\alpha_{cr}} - 2$ is proposed for design purposes to determine the minimum number of load increments in a second-order elastic analysis with a predictor-corrector solution scheme. Although a linear buckling analysis is required to calculate $AF_{\alpha_{cr}}$, computer code can be easily written to automatically calculate $P_{cr}$ and the number of load increments prior to performing the second-order analysis. The proposed equation $5AF_{\alpha_{cr}} - 2$ will save computational time when buildings have a large number of load combinations, and the cumulative total of load increments is significantly and confidently reduced when conducting all of the second-order elastic analyses.

## References


Ekhande, S.G., Selvappalam, M., Madugula, M.K.S. (1989). Stability functions for three-dimensional beam-columns, *Jour. of Struct. Eng.* 115 (2) 467-479.

EN 1993-1-1 (2005): Eurocode 3: *Design of steel structures - Part 1-1: General rules and rules for buildings*, CEN.

Galambos, T.V., Surovek, A.E. (2008). *Structural stability of steel: concepts and applications for structural engineers*, Wiley, New York.

McGuire, W., Gallagher, R. H., Ziemian, R. D. (2000). *Matrix structural analysis*, 2nd Ed., Wiley, New York.

Merchant, W. (1954). The failure load of rigid jointed frameworks as influenced by stability, *Jour. of Struct. Eng.* 32 (7) 185-190.

Standards Australia International, AS 4100 (2020): *Steel Structures*, 3rd ed.

Yang, Y.B., McGuire, W. (1986). Stiffness matrix for geometric nonlinear analysis, *Jour. of Struct. Eng.* 112 (4) 853-877. https://doi.org/10.1061/(ASCE)0733-9445(1986)112:4(853).

Ziemian, C.W., Ziemian, R.D. (2021). Efficient geometric nonlinear elastic analysis for design of steel structures: Benchmark studies, *Jour. of Constr. Steel Res.* 186 106870, https://doi.org/10.1016/j.jcsr.2021.106870.

Ziemian R.D., McGuire W. (2014) MASTAN2, Version 3.5, https://mastan2.com/.